JOURNAL OF SOLID STATE CHEMISTRY 97, 56–64 (1992)

$PbBaSrYCu_3O_7$: A "0223" Structure, Intergrowth of Single Rock Salt Layers and Triple Oxygen-Deficient Perovskite Layers; X-ray, Neutron Diffraction, and Electron Microscopy Study

T. ROUILLON, V. CAIGNAERT, M. HERVIEU, C. MICHEL, D. GROULT, AND B. RAVEAU

Laboratoire CRISMAT, ISMRa, Bd du Maréchal Juin, 14050 Caen Cedex, France

Received July 1, 1991

The structure of $PbBaYSrCu_3O_7$ has been determined by neutron and X-ray powder diffraction using a profile analysis method. The symmetry is tetragonal with space group *I4mm* and cell parameters $a = 3.8436(1)$ Å and $c = 27.426(1)$ Å. The structure of this oxide is built up from the intergrowth of single rock salt layers with triple perovskite layers. The perovskite layer is oxygen deficient and perfectly ordered according to a sequence of one layer of $Cu^{I}O_2$ sticks and two layers of CuO_5 pyramids. The ordering of copper and lead on two different sites is demonstrated, showing definitively the existence of a perfectly ordered "0223" type structure, contrary to the existence of mixed lead/copper layers proposed by previous authors. The oxygen distribution and coordination of lead and copper are compared to those observed for $Pb_2Sr_2YCu_3O_8$ and $PbBa_{0.8}Sr_{1.2}PrCeCu_3O_9$.

Introduction

The basic mechanism which describes the structure of the layered high T_c cuprates consists of an intergrowth of multiple oxygen-deficient perovskite layers with multiple rock salt-type layers (*1, 2*). This structural principle which corresponds to the general formulation $(ACuO_{3-x})_m(A'O)_n$ has been verified by neutron diffraction, X-ray diffraction, and electron microscopy for a great number of copper oxides. However, one of them, $PbBaSrYCu_3O_8$ described as a "0223" oxide, i.e., as an intergrowth of single rock salt layer with oxygen-deficient triple copper layers (*3*) has been the subject of controversy. The investigation of this phase by electron microscopy by Tokiwa *et al.* (*4*) led the authors to find a structure consisting of mixed layers of copper and lead distributed on the same crystallographic sites, leading to a "2212"-type structure. Moreover the structural problem is complicated by the fact that large amounts of oxygen can be intercalated and disintercalated in the matrix, so that the oxygen stoichiometry ranges from "O_7" to "$O_{8.5}$." In these conditions, Tokiwa *et al.* (*4, 5*) proposed the existence of univalent copper and divalent lead on the same equivalent site for the reduced phase $PbBaSrY_{(1-x)}Ca_xCu_3O_7$. However, this second model was established on the basis of high resolution images, where the authors detected a mosaic of small domains (*4, 5*), whereas such phenomena were never observed in the course of our HREM observation. Moreover, in the absence of accurate atomic coordinates, no image calcula-

0022-4596/92 $3.00

tion was performed for this HREM study (*4, 5*). In order to decide between "0223" and "2212" models we have synthesized the oxide $PbBaSrYCu_3O_7$. The present paper deals with the X-ray diffraction (XRD), neutron diffraction (N.D.), and electron microscopy study of this oxide.

Experimental

Synthesis

The oxide $PbBaSrYCu_3O_7$ was prepared by mixing and grinding PbO, $SrCuO_2$, $BaCuO_2$, Y_2O_3, and Cu_2O in stoichiometric ratios. The mixture was first heated at 830°C in a nitrogen flow containing about 1% O_2 for 3 days and quenched to room temperature. The sample was ground again, and annealed at 600°C in an argon flow for several days until the weight loss was negligible, and then slow cooled to room temperature in order to reach the stoichiometric composition "O_7."

Characterization

A systematic characterization was performed by X-ray diffraction, electron diffraction, and electron microscopy.

X-ray powder diffraction patterns were registered with a Philips PW 1050/80 (Θ-2Θ) goniometer using Cu$K\alpha$ radiation. Intensities were measured between 6° and 125° (2Θ) by steps of 0.02° (2Θ), the profile refinement was performed between 12° and 125° (2Θ) using a modified version of the DBW 3.2S program (*6*) with a pseudo-Voigt peak shape for calculation leading to the refined value of 0.487(13) for the Eta parameter. The electron diffraction was performed with a JEOL 120CX electron microscope equipped with a side entry goniometer (±60°). The high resolution electron microscopy study was carried out with a JEOL 200CX (200 KV) fitted with an objective lens of spherical aberation constant $C_s = 0.8$ mm; samples were smoothly ground, suspended in alcohol and deposited on a holey carbon film.

The neutron powder diffraction pattern was registered at room temperature on the high resolution diffractometer 3T2 at LLB (Saclay), using a wavelength of 1.2269 Å. Intensities were measured between 5.5° and 122° (2Θ) with increments of 0.05° (2Θ). The structure was refined between 11° and 122° (2Θ) with the Rietveld method using a modified version of the DBW 3.2 S program (*6*). For calculation, the peak shape was assumed to be Gaussian.

Results

Electron Diffraction and X-ray Characterization

The E.D. investigation of more than 100 crystals gave evidence of a single phase material, in agreement with the X-ray diffractograms which were indexed in a tetragonal cell with the following parameters: $a = 3.8432(1)$ Å, $c = 27.422(1)$ Å, with the reflection conditions $h + k + l = 2n$, leading to the possible space groups *I4/mmm*, $I\bar{4}m2$, *I4mm*, *I*422, *I4/m*, $I\bar{4}$, *and I*4.

No intense satellites were observed on [001] E.D. patterns (Fig. 1a) contrary to $PbBaSrYCu_3O_8$ (*3*) (Fig. 1b). However, it should be noted that very weak extra spots violate the *I*-type symmetry in some crystals. In the same way, some [100] E.D. patterns exhibit very weak diffuse streaks along **c** (Fig. 1c); the images gave evidence for the existence of some defective slices with a periodicity along **c** close to 15.7Å, i.e., of

FIG. 1. Comparison between two typical [001] E.D. patterns of (a) $PbBaSrYCu_3O_7$ and (b) $PbBaSrYCu_3O_8$. Example of one of the most disturbed crystals: (c) [100] E.D. pattern showing very weak diffuse streaks along C; (d) corresponding bright field image showing the existence of defective slice (arrowed).

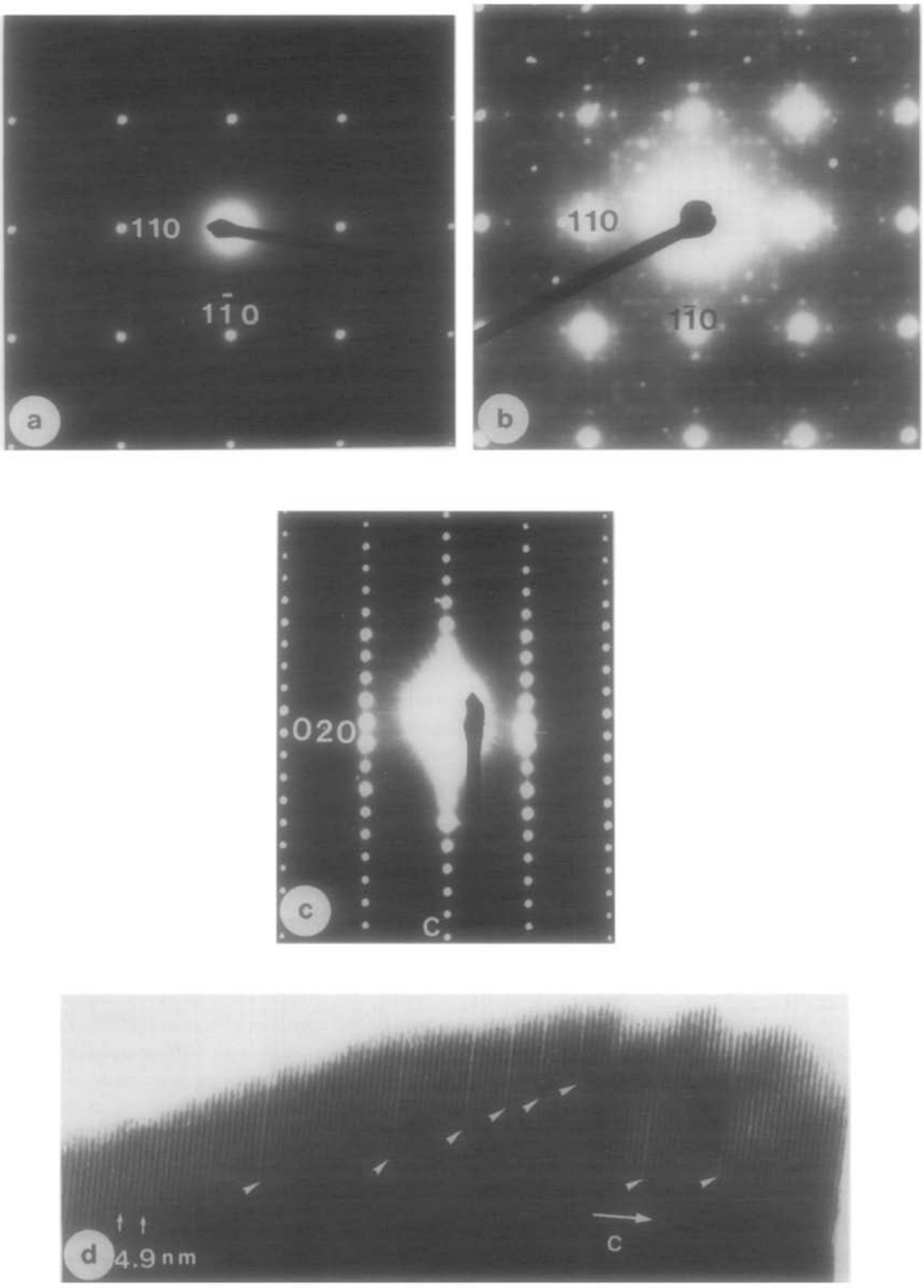
110
1$\bar{1}$0
a
110
1$\bar{1}$0
b
020
c
c
4.9 nm
d
c

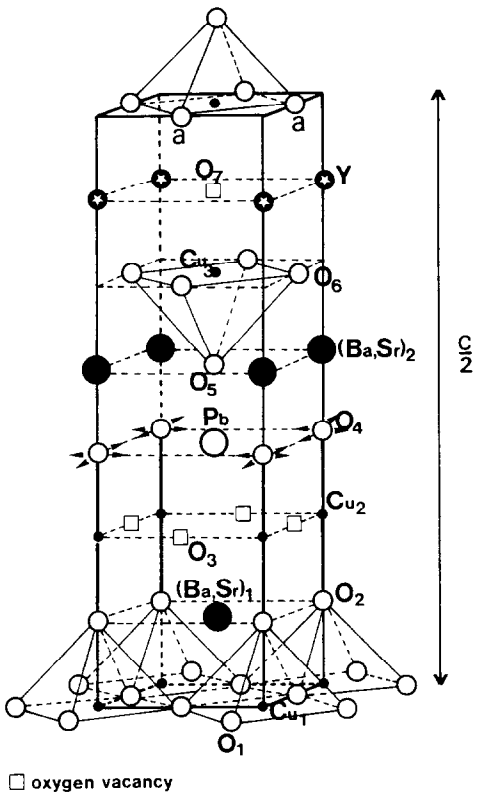

FIG. 2. Structural model of $PbBaSrYCu_3O_7$ (S.G.: *I4mm*)

$Pb_2Sr_2YCu_3O_8$-type (Fig. 1d). Thus, these first results show that the incommensurability of the structure observed for PbBaSr YCu_3O_8 (*3*) was strongly correlated to the oxygen excess, with respect to the "O_7" stoichiometry.

Structure Determination: X-ray and Neutron Powder Diffraction

In order to obtain a maximum accuracy on the atomic positions of both heavy cations and oxygen atoms, the structural parameters were refined simultaneously from X-ray and neutron diffraction data. The starting parameters were deduced from the "0223" model (Fig. 2) in which the triple oxygen-deficient perovskite layer consists of one $[Cu^{I}]_\infty$ and two $[Cu^{II}O_2]_\infty$ slabs.

The preliminary X-ray powder diffraction study was performed on the 129 *hkl* reflections allowed by the *I4mm* space group. A preferred orientation function (March's Model (*7*)) was introduced for calculation and led to the value of 0.957(3) for the refined parameter with the (001) preferred orientation direction, and to the following reliability factors: R_{wp} = 8.77%, R_{exp} = 5.68%, and R_i = 5.24%.

The refined structural parameters of the metallic atoms are given in Table I; Figure 3 shows the corresponding profile X-ray diffraction patterns. The positions of oxygen atoms are, of course, not known with accuracy, owing to the low weight of oxygen with respect to heavy cations like barium and lead. The most important result deals with the distribution of copper and lead: the refined occupancy factors of the $Cu_{(2)}$ and Pb sites show without any ambiguity that a statistical distribution of lead and copper between these two sites which would make them crystallographically equivalent is absolutely ruled out, since it would involve a dramatic increase of the *R* factors; all attempts to introduce Pb on the $Cu_{(2)}$ site and Cu on the Pb site lead to a significant increase of the reliability factors. Moreover, the $Cu_{(1)}$–$Cu_{(2)}$ and $Cu_{(3)}$–Pb distances respectively of 4.21 and 4.53 Å confirm the absence of a mirror plane perpendicular to **c**, and consequently disqualifies the *I4/mmm* space group which would arise from the statistical distribution of lead and copper between $Cu_{(2)}$ and Pb layers. The refinement of the occupancy factors of $(Ba, Sr)_{(1)}$ and $(Ba, Sr)_{(2)}$ sites shows that there exits a preferential occupancy of barium on the first sites (70%), and consecutively of strontium on the second one.

The neutron diffraction study was performed on the 225 *hkl* reflections allowed by the *I4mm* space group, leading to the following cell parameters: a = 3.8436(1) Å, c = 27.426(1) Å. The cationic and anionic positions and isotropic thermal factors were

TABLE I

$PbBaSrYCu_3O_7$ REFINED STRUCTURAL PARAMETERS FOR X-RAY POWDER DIFFRACTION

Site	Occupation	Position	x/a	y/b	z/c	B(Å^2)	τ (occ. ratio)
$Cu_{(1)}$	Cu^{2+}	2*a*	0	0	0	0.29(10)[d]	1.00[b]
$(Ba, Sr)_{(1)}$	Ba^{2+}/Sr^{2+}	2*a*	$\frac{1}{2}$	$\frac{1}{2}$	0.0689(5)	0.15(12)[e]	0.66(3)/0.34(3)
$Cu_{(2)}$	Cu^{+}/Pb^{2+}	2*a*	0	0	0.1535(4)	0.29(10)[d]	1.00(1)/0.00(1)
Pb	Cu^{+}/Pb^{2+}	2*a*	$\frac{1}{2}$	$\frac{1}{2}$	0.2143(4)	0.44(09)	0.01(2)/0.99(2)
$(Ba, Sr)_{(2)}$	Ba^{2+}/Sr^{2+}	2*a*	0	0	0.3109(6)	0.15(12)[e]	0.27(4)/0.73(4)
$Cu_{(3)}$	Cu^{2+}	2*a*	$\frac{1}{2}$	$\frac{1}{2}$	0.3797(4)	0.29(10)[d]	1.00[b]
Y	Y^{3+}	2*a*	0	0	0.4398(4)	0.29(10)[d]	1.00[b]
$O_{(1)}$	O^{2-}	4*b*	0	$\frac{1}{2}$	−0.0052(9)	1.00[a]	1[a]
$O_{(2)}$	O^{2-}	2*a*	0	0	0.0932(16)	1.00[a]	1[a]
$O_{(3)}$	O^{2-}	4*b*	0	$\frac{1}{2}$	0.1535[f]	1.00[a]	0[a]
$O_{(4)}$[c]	O^{2-}	8*d*	0.143(11)	0	0.2153(25)	1.00[a]	0.25[a]
$O_{(5)}$	O^{2-}	2*a*	$\frac{1}{2}$	$\frac{1}{2}$	0.2924(17)	1.00[a]	1[a]
$O_{(6)}$	O^{2-}	4*b*	0	$\frac{1}{2}$	0.3922(14)	1.00[a]	1[a]
$O_{(7)}$	O^{2-}	2*a*	$\frac{1}{2}$	$\frac{1}{2}$	0.4398[f]	1.00[a]	0[a]

Note. Space group *I4mm* (*n*°107), $Z = 2$, $a = b = 3.8432(1)$ Å, $c = 27.422(1)$ Å; $R_p = 6.74\%$, $R_{wp} = 8.77\%$, $R_{exp} = 5.68\%$, $R_I = 5.24\%$, $R_f = 4.18\%$.

[a] Fixed parameters.

[b] Refined and then fixed.

[c] Deviated from the (2*a*) position [0, 0, 0.2153].

[d] Refined simultaneously.

[e] Refined simultaneously.

[f] Empty positions at $(Cu, Pb)_{(1)}$ and Y level.

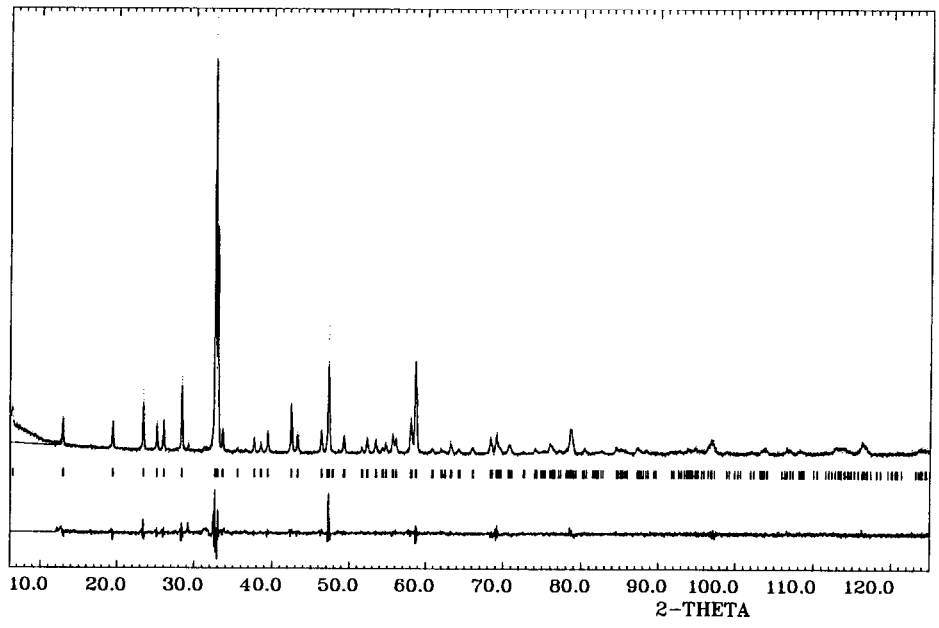

FIG. 3. X-ray powder diffraction patterns of $PbBaSrYCu_3O_7$: experimental, calculated, and difference (OBS-CALC) profiles.

TABLE II

$PbBaSrYCu_3O_7$ REFINED STRUCTURAL PARAMETERS FOR NEUTRON POWDER DIFFRACTION

Atom	Position	x/a	y/b	z/c	B(Å^2)	τ (occ. ratio)
$Cu_{(1)}$	2*a*	0	0	0	0.39(4)[d]	1[a]
$(Ba, Sr)_{(1)}$	2*a*	$\frac{1}{2}$	$\frac{1}{2}$	0.0704(6)	0.58(6)[e]	0.7/0.3[a]
$Cu_{(2)}$	2*a*	0	0	0.1533(4)	1.74(17)	1[a]
Pb	2*a*	$\frac{1}{2}$	$\frac{1}{2}$	0.2152(3)	1.24(11)	1[a]
$(Ba, Sr)_{(2)}$	2*a*	0	0	0.3119(5)	0.58(6)[e]	0.3/0.7[a]
$Cu_{(3)}$	2*a*	$\frac{1}{2}$	$\frac{1}{2}$	0.3789(2)	0.39(4)[d]	1[a]
Y	2*a*	0	0	0.4395(6)	0.48(6)	1[a]
$O_{(1)}$	4*b*	0	$\frac{1}{2}$	0.0079(4)	0.85(17)	1.00[b]
$O_{(2)}$	2*a*	0	0	0.0874(5)	1.31(24)	1.00[b]
$O_{(3)}$	4*b*	0	$\frac{1}{2}$	0.1533[g]	1[c]	0.00(2)
$O_{(4)}$[f]	8*d*	0.1366(24)	0	0.2190(6)	0.97(30)	0.25(1)
$O_{(5)}$	2*a*	$\frac{1}{2}$	$\frac{1}{2}$	0.2929(6)	1.27(20)	1.00[b]
$O_{(6)}$	4*b*	0	$\frac{1}{2}$	0.3869(4)	0.45(14)	1.00[b]
$O_{(7)}$	2*a*	$\frac{1}{2}$	$\frac{1}{2}$	0.4395[g]	1[c]	0.01(1)

Note. Space group *I4mm* ($n°107$), $Z = 2$, $a = b = 3.8436(1)$ Å, $c = 27.426(1)$ Å; $R_p = 6.39\%$, $R_{wp} = 7.88\%$, $R_{exp} = 4.76\%$, $R_i = 5.15\%$, $R_f = 4.55\%$.

[a] Fixed from the X-ray powder diffraction.

[b] Refined in first step and then fixed.

[c] Fixed parameters.

[d] Refined simultaneously.

[e] Refined simultaneously.

[f] Deviated from the (2*a*) position [0, 0, 0.2190].

[g] Empty positions at $Cu_{(2)}$ and Y level.

refined simultaneously. After refinements five oxygen sites ($O_{(1)}$, $O_{(2)}$, $O_{(4)}$, $O_{(5)}$, and $O_{(6)}$) were found to be fully occupied. $O_{(1)}$ and $O_{(6)}$ are respectively at the level of the copper atoms $Cu_{(1)}$ and $Cu_{(3)}$, leading to $[Cu_{(1)}O_2]_\infty$ and $[Cu_{(3)}O_2]_\infty$ layers. $O_{(2)}$, $O_{(4)}$, and $O_{(5)}$ are at the level of the lead and alkaline earth cations, leading to $[PbO]_\infty$ and $[(Ba, Sr)O]_\infty$ layers. Two sites are found to be empty: $O_{(3)}$ and $O_{(7)}$. $O_{(7)}$ is at the level of the yttrium cations leading to the formation of the classical YO_8 fluorite type cage for the ions intercalated between the pyramidal layers. $O_{(3)}$ is at the level of the $Cu_{(2)}$ layers, involving for this cation a twofold coordination, in agreement with its oxidation state, +1. According to the results obtained for similar structure, $Pb_2Sr_2YCu_3O_8$ (*8*), $Pb_2Ba_2YCu_3O_8$ (*9*), and $PbBa_{0.8}Sr_{1.2}PrCeCu_3O_9$ (*10*), the high isotropic thermal factor of $O_{(4)}$ in the (2a) site, led us to introduce a splitting of this site into an (8*d*) site with an occupancy factor of $\frac{1}{4}$. The atomic coordinates were then easily refined leading to a significant decrease of the R factors: $R_{wp} = 7.88\%$, $R_{exp} = 4.76\%$, and $R_i = 5.15\%$. The final structural parameters are given in Table II, and the corresponding interatomic distances in Table III. They show the good agreement with X-ray results as to the positions of metallic atoms, especially for lead and barium. The comparison of the calculated and observed patterns (Fig. 4) shows that their difference is almost perfect, except for the 020 and 040 reflections, which exhibit stronger intensities than the calculated ones; the existence of some irregular defective slices of $Pb_2(Ba, Sr)_2YCu_3O_8$-type along the **c** axis is assumed to be responsible of this phe-

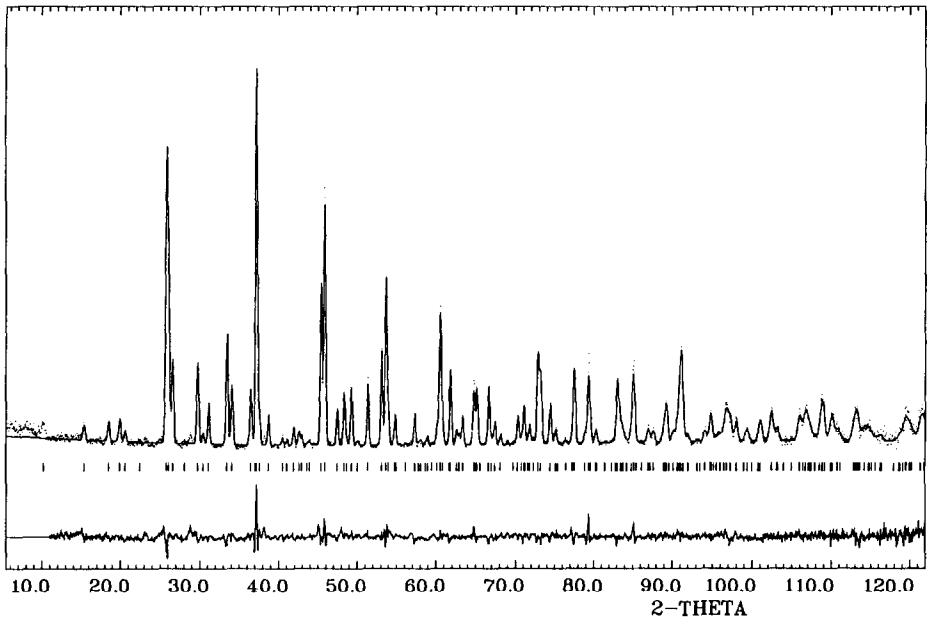

FIG. 4. Neutron powder diffraction patterns of $PbBaSrYCu_3O_7$: experimental, calculated, and difference (OBS-CALC) profiles.

nomenon owing to its closely related cell parameters.

Description of the Structure and Discussion

These results demonstrate without any ambiguity that $PbBaYSrCu_3O_7$ is a "0223" structure and not a "2212"-type oxide. The triple oxygen-deficient perovskite layers forming the structure consist of double pyramidal copper layers $[Cu_2O_5]_\infty$ and of $[CuO]_\infty$ layers of Cu^I–O_2 sticks. The single rock salt layers are formed of one $[PbO]_\infty$ layer and one $[(Ba_{0.3}Sr_{0.7})O]_\infty$ layer.

Thus the $Cu_{(2)}$ site is fully occupied by copper and the Pb site by lead, in agreement with our HREM images (Fig. 5), which attest to the absence of mosaic domains.

The splitting of 0.53 Å of the $O_{(4)}$ sites shows that there exists a disordering of oxygen in the $[PbO]_\infty$ layer (Fig. 6); such a phenomenon previously observed for $Pb_2Sr_2YCu_3O_8$ (*8*), $Pb_2Ba_2YCu_3O_8$ (*9*) and $PbBa_{0.8}Sr_{1.2}PrCeCu_3O_9$ (*10*) is characteristic of adjacent $[Pb^{II}O]_\infty$ and $[Cu^IO]_\infty$ layers. Indeed, Pb(II), forms with two $O_{(4)}$, and one $O_{(5)}$ oxygen atoms three short bonds ranging from 2.132 to 2.378 Å and two much larger ones of 3.113 Å with two $O_{(4)}$ oxygen atoms (Table III) so that its coordination PbO_3L can be described as tetrahedral, its $6s^2$ lone pair L extending in the perpendicular direction to the plane formed by three oxygen atoms toward the $[Cu^IO]_\infty$ empty layer (Fig. 7). Bond valence calculations (*13*) give respectively +1.04 and +2.03 for the $Cu_{(2)}$ and Pb sites and confirm their oxidation states.

The CuO_5 pyramids exhibit a regular basal plane with four equal Cu–O distances of 1.93 Å and an apical Cu–O distance of 2.36 to 2.40 Å (Table III) intermediate between that observed in $YBa_2Cu_3O_7$ (*11*) and in thallium superconductive cuprates (*12*).

The eightfold coordination of yttrium is

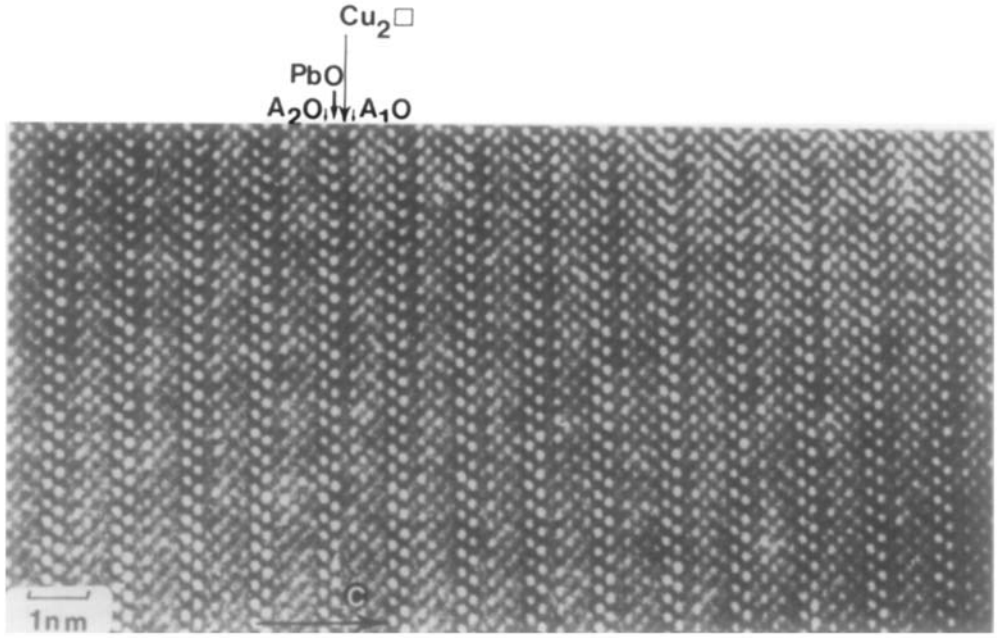

FIG. 5. Typical [010] HREM image of $PbBaSrYCu_3O_7$: absence of mosaic domains and evenness of the contrast.

found to be symmetric with eight distances of 2.40 Å in the fluorite cage (Table III). One also observes a nonlinear coordination of the O–$Cu^{(I)}$–O bonds which exhibit an angle of 164° (Fig. 7). This phenomena was also observed for $Pb_2Sr_2Y_{1-x}Ca_xCu_3O_8$ (*8*), $Pb_2Ba_2YCu_3O_8$ (*9*), and for $PbBa_{0.8}Sr_{1.2}PrCeCu_3O_9$ (*10*). The nonlinearity of copper–oxygen bonding might be due to the proximity of the $6s^2$ lone pair of Pb(II), which plays the role of a ligand and consequently disturbs the anionic arrangement around Cu(I).

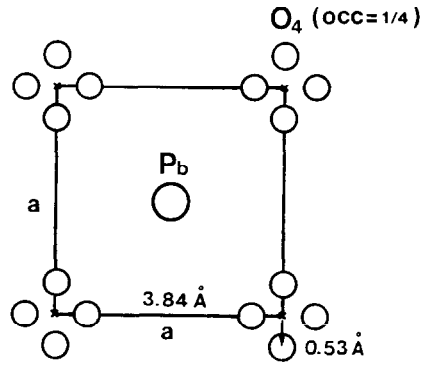

FIG. 6. The splitting of the $O_{(4)}$ sites in the $[PbO]_\infty$ layers.

TABLE III

INTERATOMIC DISTANCES (IN Å) ALLOWED BY NEUTRON POWDER DIFFRACTION IN $PbBaSrYCu_3O_7$

$Cu_{(1)}$–$O_{(1)}$ 1.934(1)[×4]	(Ba, Sr)$_{(2)}$–$O_{(4)}$ 2.60(2) [×1]
$Cu_{(1)}$–$O_{(2)}$ 2.40(1) [×1]	(Ba, Sr)$_{(2)}$–$O_{(5)}$ 2.767(4) [×4]
	(Ba, Sr)$_{(2)}$–$O_{(6)}$ 2.82(1) [×4]
(Ba, Sr)$_{(1)}$–$O_{(1)}$ 2.88(1) [×4]	
(Ba, Sr)$_{(1)}$–$O_{(2)}$ 2.758(4) [×4]	$Cu_{(3)}$–$O_{(6)}$ 1.934(1) [×4]
	$Cu_{(3)}$–$O_{(5)}$ 2.36(2) [×1]
$Cu_{(2)}$–$O_{(2)}$ 1.81(2) [×1]	
$Cu_{(2)}$–$O_{(4)}$ 1.88(2) [×1]	Y–$O_{(6)}$ 2.40(1) [×4]
	Y–$O_{(1)}$ 2.40(1) [×4]
Pb–$O_{(5)}$ 2.13(2) [×1]	
Pb–$O_{(4)}$ 2.378(6) [×2]	Angle between the Cu^I–O:
3.113(7) [×2]	$O_{(2)}$–$Cu_{(2)}$–$O_{(4)}$ 164°

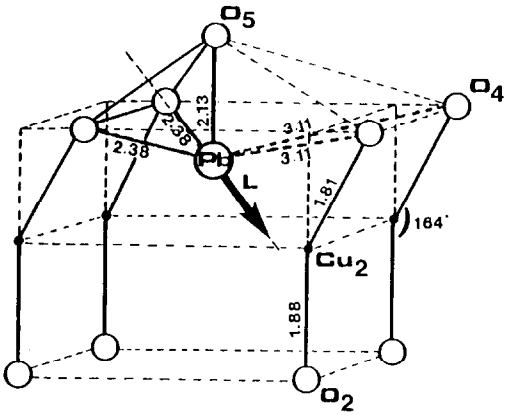

FIG. 7. Environment of Pb and $Cu_{(2)}$ showing the tetrahedral coordination of PbO_3L; the lone pair, L, is symbolized by a large black arrow. Distances are in angstroms. Note the nonlinear coordination of the $O_{(2)}$–$Cu^{I}_{(2)}$–$O_{(4)}$ sticks, which exhibit an angle of 164°.

Concluding Remarks

The X-ray and neutron diffraction study of $PbBaSrYCu_3O_7$ definitively shows that this oxide exhibits a "0223" structure built up from triple oxygen-deficient perovskite layers intergrown with single rock salt layers. No statistical distribution of lead and copper on the same sites must be considered. The ordering of oxygens and vacancies on the anionic lattice leading to layers of $[Cu^{(I)}O_2]$ stick shows the great similarity of this structure with the $Pb_2Sr_2Y_{1-x}Ca_xCu_3O_8$ structure, from which it differs by the elimination of one $[PbO]_\infty$ layer out of two along **c**. In the same way, $PbBaSrYCu_3O_7$ structure can be deduced from that of $YBa_2Cu_3O_6$ by introduction of one $[PbO]_\infty$ layer per cell. Thus, this framework is intermediate between the two structural types $YBa_2Cu_3O_6$ and $Pb_2Sr_2Y_{1-x}Ca_xCu_3O_8$. The great ability of $PbBaSrYCu_3O_7$ to intercalate oxygen suggests that the parent oxide PbBaYSr Cu_3O_8, which exhibits an incommensurate structure, should differ from this oxide mainly by a modulated displacement of cations and oxygen atoms within the different layers, but not by a migration of cations from one layer to the other.

Acknowledgment

We thank Mme F. Bouree of the LLB (Saclay) for the neutron diffraction measurements.

References

1. B. RAVEAU, C. MICHEL, AND M. HERVIEU, *Solid State Ionics* **32,** 1035 (1989).
2. B. RAVEAU, C. MICHEL, M. HERVIEU, D. GROULT, AND J. PROVOST, *MRS* **156,** 129 (1989).
3. T. ROUILLON, R. RETOUX, D. GROULT, C. MICHEL, M. HERVIEU, J. PROVOST, AND B. RAVEAU, *J. Solid State Chem.* **78,** 322 (1989).
4. A. TOKIWA, T. OKU, M. NAGOSHI, M. KIKUCHI, K. HIRAGA, AND Y. SYONO, *Physica C* **161,** 459 (1989).
5. A. TOKIWA, N. NAGOSHI, T. OKU, N. KOBAYASHI, M. KIKUCHI, K. HIRAGA, AND Y. SYONO, *Physica C* **168,** 285 (1990).
6. D. B. WILES AND R. A. YOUNG, *J. Appl. Crystallogr.* **14,** 149 (1981).
7. A. MARCH, *Z. Kristallogr.* **81,** 285 (1932); W. A. Dollase, *J. Appl. Crystallogr.* **19,** 267 (1986).
8. R. J. CAVA, M. MAREZIO, J. J. KRAJEWSKI, W. F. PECK, JR., A. SANTORO, AND F. BEECH, *Physica C* **157,** 272 (1989).
9. W. T. FU, H. W. ZANDBERGEN, W. G. HAIJE, AND L. J. DE JONGH, *Physica C* **159,** 210 (1989).
10. T. ROUILLON, V. CAIGNAERT, C. MICHEL, M. HERVIEU, D. GROULT, AND B. RAVEAU, *J. Solid State Chem.* **96** (1992).
11. J. J. CAPPONI, C. CHAILLOUT, A. W. HEWAT, P. LEJAY, M. MAREZIO, N. NGUYEN, B. RAVEAU, J. L. SOUBEYROUX, J. L. THOLENCE, AND R. TOURNIER, *Europhys. Lett.* **3,** 1301 (1987).
12. C. MICHEL, E. SUARD, V. CAIGNAERT, C. MARTIN, A. MAIGNAN, M. HERVIEU, AND B. RAVEAU, *Physica C,* **178,** 29 (1991).
13. I. D. BROWN AND D. ALTERMATT, *Acta Crystallogr., Sect. B: Struct. Sci.* **41,** 244 (1985).